




Article

Dynamic Model for Biomass and Proteins Production by Three *Bacillus Thuringiensis* ssp *Kurstaki* Strains

Tatiana Segura Monroy ¹, Nouha Abdelmalek ², Souad Rouis ³ , Mireille Kallassy ⁴, Jihane Saad ^{4,5}, Joanna Abboud ^{4,5}, Julien Cescut ⁵, Nadia Bensaid ², Luc Fillaudeau ¹  and César Arturo Aceves-Lara ^{1,*} 

- ¹ Toulouse Biotechnology Institute, Bio & Chemical Engineering, Université de Toulouse, F-31077 Toulouse, France; seguramo@insa-toulouse.fr (T.S.M.); luc.fillaudeau@insa-toulouse.fr (L.F.);
 - ² Laboratoires Pharmaceutiques MédiS, B.P 206 Nabeul 8000, Tunisia; nouha_abdelmalek@yahoo.com (N.A.); nadia.bensaid@labomedis.com (N.B.)
 - ³ Centre of Biotechnology of Sfax, B.P 1177 Sfax 3018, Tunisia; souad.rouis@cbs.rnrt.tn
 - ⁴ Faculty of Sciences, Saint-Joseph University, Riad El Solh, Beirut 1004 2020, Lebanon; mireille.kallassy@usj.edu.lb (M.K.); jihane.saad@inrae.fr (J.S.); joanna.abboud-1@inrae.fr (J.A.)
 - ⁵ Toulouse White Biotechnology (UMS INRAE/INSA/CNRS), 135 Avenue de Rangueil, F-31077 Toulouse, France; Julien.Cescut@inrae.fr
- * Correspondence: seguramo@etud.insa-toulouse.fr

Abstract: *Bacillus thuringiensis* is a microorganism used for the production of biopesticides worldwide. In the present paper, different kinetic models were analyzed to study and compare three different strains of *Bt* ssp *kurstaki* (LIP, BLB1, and HD1). Bioperformances (vegetative cell, spore, substrate, and protein) and successive culture phases (oxidative growth, limitation and sporulation, and protein release) were depicted with an overarching aim to estimate total protein productivity, yield, and titer. In the end, two models were calibrated using experimental dataset (11 batches culture in 3 L bioreactor with semisynthetic medium), subsequently validated, and statistically compared. Both models satisfactorily followed the dynamics of the experimental data. Finally, a dynamic model was selected following the Akaike information criterion (AIC).

Keywords: *B. thuringiensis* *kurstaki*; biopesticides; kinetic parameters; dynamic model



Citation: Monroy, T.S.; Abdelmalek, N.; Rouis, S.; Kallassy, M.; Saad, J.; Abboud, J.; Cescut, J.; Bensaid, N.; Fillaudeau, L.; Aceves-Lara, C.A. Dynamic Model for Biomass and Proteins Production by Three *Bacillus Thuringiensis* ssp *Kurstaki* Strains. *Processes* **2021**, *9*, 2147. <https://doi.org/10.3390/pr9122147>

Academic Editor: Philippe Bogaerts

Received: 27 October 2021

Accepted: 24 November 2021

Published: 28 November 2021

Publisher's Note: MDPI stays neutral with regard to jurisdictional claims in published maps and institutional affiliations.



Copyright: © 2021 by the authors. Licensee MDPI, Basel, Switzerland. This article is an open access article distributed under the terms and conditions of the Creative Commons Attribution (CC BY) license (<https://creativecommons.org/licenses/by/4.0/>).

1. Introduction

B. thuringiensis is a facultative anaerobic Gram-positive sporulating bacterium, frequently used in the production of some biopesticides and as a source of genes for transgenic expression in plants [1]. It usually inhabits different environments, among which soil, settled dust, insects, water, and others have been identified [2]. *B. thuringiensis* has been shown to be toxic to various organisms, such as lepidopterans, coleopterans, dipterans, or nematodes, but is considered safe for mammals. Thus, the products based on *B. thuringiensis* (*Bt*) provide effective and environmentally benign control of several insects in agricultural, forestry, and disease-vector applications [3]. This insecticidal activity is mainly due to the production of some intracellular inclusions (called σ -endotoxins) during the sporulation phase of *B. thuringiensis* cells.

Most of the biopesticides distributed in the world are mainly based on *Btk*. HD1 strain. However, two recent strains, identified as *Btk*. LIP (from Lebanese soil), and BLB1 (from Tunisian soil), have been isolated and described to be more efficient than HD1 [4], and, therefore, will be studied in this work.

Due to the several changes of cell physiology during the σ -endotoxins production bioprocess (exponential growth, formation of inclusion, formation of spore, lysis), *B. thuringiensis* culture is considered a laborious process. Although one possibility to optimize *B. thuringiensis* culture is through mathematical models, there are not many mathematical models that describe the dynamics of the growth phases of *B. thuringiensis* culture [5]. Holmberg and Sievanen [6] proposed a model based on Monod kinetics to describe the

relationship between cell growth and toxin production. Later, Rivera et al. (1999) [7] showed the Monod model limitations when they tried to describe the biomass diversity of *B. thuringiensis*. In their model, they assumed the presence of two kind of cells in the *B. thuringiensis* culture; those available to multiply, and those that have become spores. Thus, they divided them between the biomass of the vegetative cells and the biomass of the spore-forming cells. In addition, they used the Monod model to describe the relationship between vegetative cell growth and substrate concentration, as did Holmberg and Sievanen [6].

Furthermore, Popovic et al. [8] proposed a model that considered a minimum level of poly- β -hydroxy butyric acid (PHB) required in cells at the beginning of sporulation for efficient sporulation and endotoxins productions. Additionally, they used Contois kinetics to describe the growth of the cells, considering that this model fits better to the experimental data than the expression of Monod.

Therefore, this work proposes a dynamic model for *B. thuringiensis*. Section 2 describes experimental data and the dynamic model for *B. thuringiensis*. The simulation results and the performance evaluation are shown in Section 3. Finally, conclusions and perspectives close this paper.

2. Materials and Methods

The materials and methods used to generate the set of experimental data are described in this section. Then, experimental data are introduced, and assumption and formulation of models are explained.

2.1. Microorganism and Culture Media

Three *B. thuringiensis* ssp. *kurstaki* strains were used in the present work: a Lebanese strain LIP [4], a Tunisian strain BLB1 [9], and HD1 strain used as a reference (industrial gold standard) [10]. Luria broth (LB) medium was used for inoculum production, whereas a semisynthetic medium (SSM), defined by Sarrafzadeh et al. [11], was used for fermentation assays. Their compositions ($\text{g}\cdot\text{L}^{-1}$) are described in Table 1. For the SSM, concentrated glucose (Sol 2) and all salts solutions (Sol 3–5) were prepared and sterilized separately and added before inoculation to the rest of the medium (Sol 1) previously sterilized.

Table 1. Semisynthetic and Luria broth media composition ($\text{g}\cdot\text{L}^{-1}$).

Sol	Components	Semisynthetic (SSM)	LB
1	Peptone	-	10
	NaCl	-	5
	Yeast Extract	0.5	5
	Casein acid hydrolysate	4.5	-
	$(\text{NH}_4)_2\text{SO}_4$	6	-
	K_2HPO_4	1.4	-
	KH_2PO_4	1.4	-
2	Glucose	5	-
3	$\text{MgSO}_4, 7\text{H}_2\text{O}$	0.61	-
4	$\text{CaCl}_2, 2\text{H}_2\text{O}$	0.332	-
5	$\text{MnSO}_4, \text{H}_2\text{O}$	0.006	-

2.2. Inoculum Preparation

Inocula were prepared by transferring cells from nutrient agar slants into 10 mL of LB medium and incubated overnight at 30 °C in a rotary shaker set at 200–230 rpm. Aliquots

corresponding to an initial OD₆₀₀ = 0.15 were used to inoculate 1 L Erlenmeyer flasks containing 100 mL LB medium. After 10–12 h of incubation at 30 °C, in a rotary shaker set at 200–230 rpm, the OD₆₀₀ was determined. The culture broth was used to inoculate the bioreactor containing the studied media to start with an initial OD₆₀₀ of 0.15.

2.3. Culture Conditions

Several fermentations were conducted over 48 h in batch mode at 30 °C in a 3 L Biostat B plus fermenter (Sartorius, Göttingen, Germany) containing 1.8 L of the SSM medium and with continuous regulation of pH at 6.8 using 1 M H₂SO₄ and 3 M NaOH. Dissolved oxygen was continuously monitored by an optical oxygen sensor and maintained at 25% pO₂-sat with a constant aeration rate (VVM = 10 with Q_{air} = 0.18 min·L⁻¹) and variable stirring (from 250 to 1200 rpm). Foaming was controlled using an antifoam (Emultrol DFM DV-14 FG), through the fermentation process.

2.4. Analysis and Sampling Strategy

Several samples were collected from the *Bt* broth during experiments, and substrate, biomass, and product analyses (glucose, cell and spore counting, protein) were conducted to determine biokinetics.

2.4.1. Detection of Sporulation

The diverse cell states were distinguished, during the fermentation process, based on their morphological differences and the refractile nature of the endospores, using a phase contrast microscope (ZeissPrima Pro, Paris, France, ×100 oil).

2.4.2. Biomass Analyses

Cells and Spores Counts

The follow-up of the biopesticides production was checked by estimating viable cell counts (VC) and spore counts (SC) by plate counts. To determine VC and SC, the withdrawn samples were serially diluted, spread on LB plates and incubated at 30 °C for 16–18 h. For determining SC, the appropriately diluted samples were heated at 85 °C for 15 min and cooled for 5 min before spreading onto LB plates. Number of colonies should be between 20 and 300 to be acceptable. All analyses were realized in triplicate.

Cell Dry Weight

A known amount of sample (1 to 20 mL) was filtered via nitrocellulose membrane (0.2 µm) and the membrane was then dried at 70 °C (24 h). Biomass dry weight is determined by differential weighing of the filter before the filtration and after filtration and drying.

Quantification of Proteins Production

In order to estimate the concentration of total proteins (mainly composed of δ-endotoxin) produced during the fermentation, 1 mL sample was centrifuged at 13,000 rpm for 5 min at 4 °C. The supernatant was collected for other analysis and the pellet was washed twice with cold NaCl 1M and four times with cold water. The protein crystal was then dissolved in 0.05 N NaOH for 2 to 3 h at 30 °C in a rotary shaker (200 rpm). The suspension was then centrifuged at 13,000 rpm for 5 min, and the supernatant containing the solubilized proteins was recuperated.

The concentration of the proteins in this supernatant was determined by Bradford assay [12] using bovine serum albumin (BSA) as a protein standard. Absorbances were measured after 10 min at 595 nm (2300 EnSpire Multilabel Plate Reader). The obtained value was the average of three measures of the same sample (microwell plate). Considering our protocol, protein concentration estimates the total protein production after separation but not specifically the δ-endotoxin, even if it is the dominant fraction.

Sugar Analysis

The sugar concentrations were determined using HPLC-UV. The HPLC assays were performed using an Ultimate 3000 RSLC/MWD/RI/CAD. A mobile phase of 5 mM H₂SO₄ with a flow rate of 0.6 mL·min⁻¹ was used. The mobile phase was filtered and degassed through a 0.2 µm cellulose nitrate membrane. The samples and standards were also filtered before injection into the HPLC.

2.5. Experimental Data

Between three to four batch cultures per strain were carried out (Table 2). Two batches per strain were used to perform parameter calibration, and between one and two batches were used to validate the models. The experimental datasets for each strain are presented in Figures 1–3. It is relevant to indicate that in batch 07, dry matter measurement was estimated by OD600nm for exponential growth phase.

Table 2. Batches culture carried out per strain.

Strain	Batch
<i>Btk.</i> HD1	B03, B04, B07
<i>Btk.</i> BLB1	B01, B02, B05, B06
<i>Btk.</i> LIP	B08, B09, B10

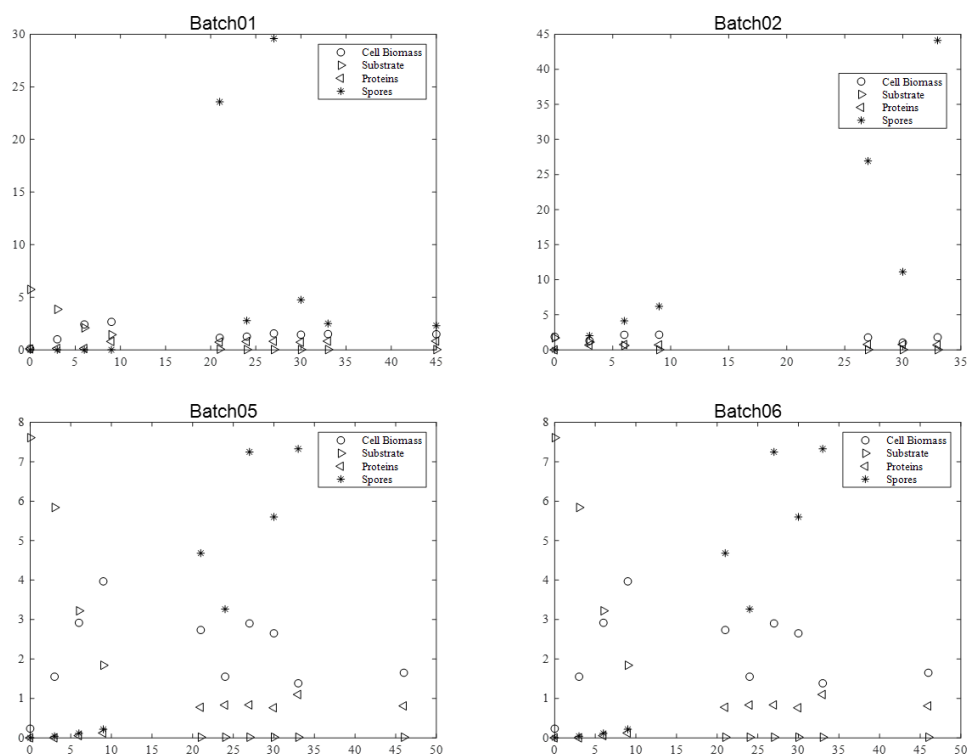


Figure 1. Evolution of cell biomass, spores, substrate, and protein content as a function of time with BLB1 strain (batches: 01, 02, 05, and 06).

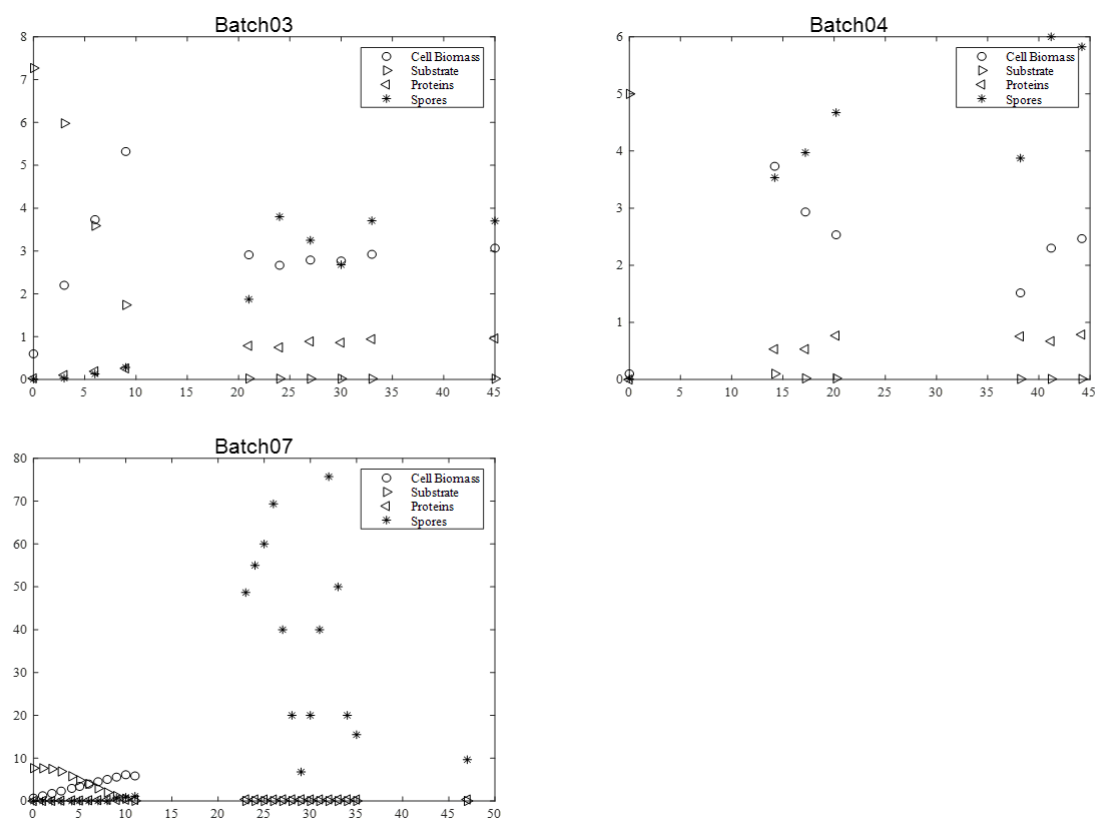


Figure 2. Evolution of cell biomass, spores, substrate, and protein content as a function of time with HD1 strain (batches: 03, 04, and 07).

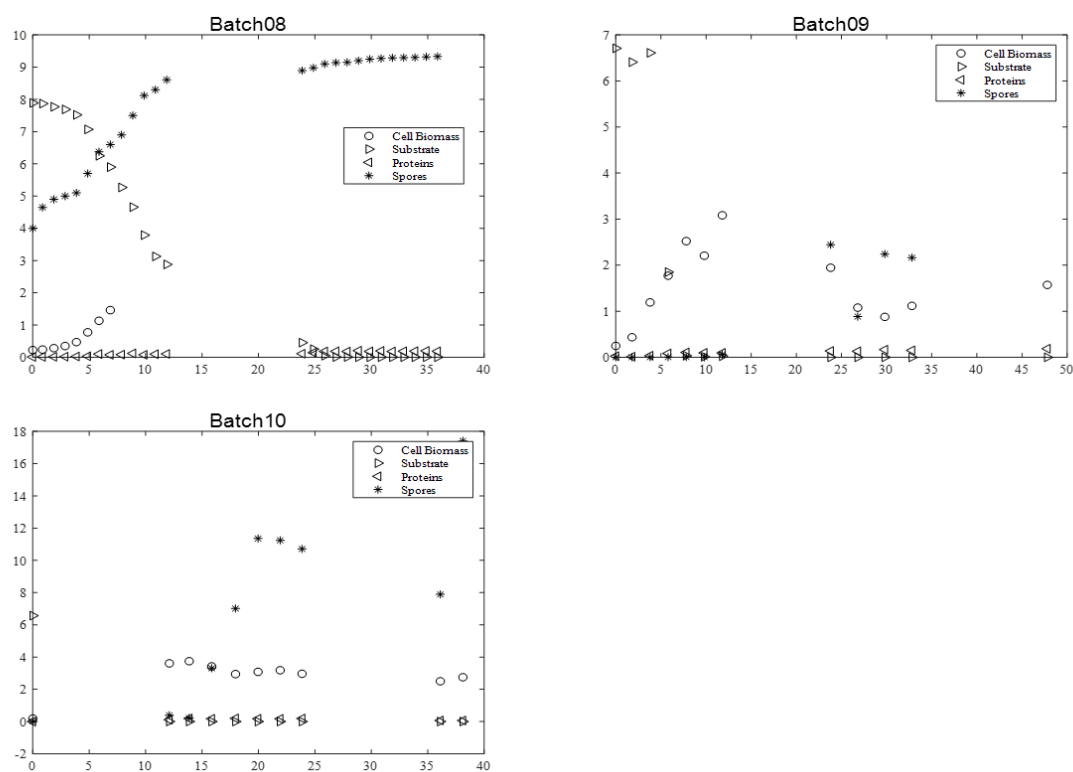


Figure 3. Evolution of cell biomass, spores, substrate, and protein content as a function of time with LIP strain (batches: 08, 09, and 10).

During all cultures, several milestones should be identified: (i) the maximum cell biomass production, (ii) substrate depletion, (iii) full sporulation informing about proteins production, and (iv) its release in supernatant due to full cell lysis.

2.5.1. *Btk*. BLB1 Strain

For the BLB1 strain, data were taken from four batches (01, 02, 05, and 06). Figure 1 presents the graphical experimental data. Batch 11 was used to validate the model.

The maximum biomass concentration was reached after approximately 10 h culture for the four batches, and then began to decrease. As expected, this time approximately coincided with the substrate depletion, corresponding to a glucose concentration close to $0 \text{ g}\cdot\text{L}^{-1}$. In addition, the concentration of spores began to increase at this moment, since the limitation of the substrate induced their formation. After 20 h, sporulation reached a plateau value. Cell lysis was fully achieved after 30 h, as indicated by protein release into supernatant. Finally, protein content reached around $0.8\text{--}1 \text{ g}\cdot\text{L}^{-1}$ with BLB1 stain.

2.5.2. *Btk*. HD1 Strain

Similar data and milestones were obtained for the HD1 strain (Figure 2). Around 10 h, maximum biomass concentration and substrate depletion were reached. However, in batch 07, no values were recorded for the biomass concentration after exponential growth phase due to technical misplaced measurements. After 20 h, sporulation rate was achieved, and protein content plateaued after 30 h. Final protein content was around $0.8\text{--}1 \text{ g/L}$, except for batch 07 (0.4 g/L).

2.5.3. *Btk*. LIP Strain

Figure 3 presents identical variables and leads to identify the same milestones and critical time as described above with *Btk*. BLB1 and HD1 strains. LIP strain exhibited the lowest protein concentration, close to 0.2 g/L . This result could be explained by a lower cell lysis rate; therefore, protein crystals were not released in the supernatant.

2.5.4. Model Assumptions

The main features of dynamic models include the key parameters describing bioperformances (vegetative cell, spores, substrate, proteins) and associated kinetics, considering successive phases (oxidative growth, limitation, sporulation, and protein release), during bioproduction. The mass balance equations on each compound are shown in Equations (1), (2), (4)–(7). Equation (1) represents the evolution of biomass concentration with respect to time, while the relationship between bacterial growth and substrate consumption is shown in Equations (1) and (2).

$$\frac{dX}{dt} = \mu * X - k_d * X \quad (1)$$

$$\frac{dS}{dt} = -\frac{\mu * X}{Y_1} \quad (2)$$

where X is the biomass concentration ($\text{g}\cdot\text{L}^{-1}$), S is the concentration of substrate ($\text{g}\cdot\text{L}^{-1}$), Y_1 is the yield coefficient between the biomass and the substrate (gBiomass/gGlucose), and k_d is the death rate (h^{-1}).

The cell growth process is represented by the Contois expression, as follows:

$$\mu = \mu_{\max} \frac{S}{(K_c * X) + S} \quad (3)$$

where μ is the specific growth rate (h^{-1}) and μ_{\max} is the maximum specific growth rate (h^{-1}), a constant defined for a substrate concentration; X_1 is the concentration of biomass ($\text{g}\cdot\text{L}^{-1}$); S_1 is the concentration of glucose ($\text{g}\cdot\text{L}^{-1}$); and K_c is a saturation constant.

Equations (4)–(7) show the mass balance for proteins and spores. In the first model, proteins and spores are correlated with biomass (Model 1). In the second model, α and

β parameters were used to unassociated proteins and spores from biomass production (Model 2). The corresponding models are shown in Equations (4) and (5) (Model 1) and Equations (6) and (7) (Model 2).

Model 1

$$\frac{dPro}{dt} = \frac{X1 \cdot Y2}{Y1} \quad (4)$$

$$\frac{dSpo}{dt} = \frac{X1 \cdot Y3}{Y1} \quad (5)$$

Model 2

$$\frac{dPro}{dt} = \frac{X1 \cdot Y2}{Y1} + \alpha \quad (6)$$

$$\frac{dSpo}{dt} = \frac{X1 \cdot Y3}{Y1} + \beta \quad (7)$$

where Pro is the protein concentration ($\text{g} \cdot \text{L}^{-1}$), Spo is the spores concentration ($\text{CFU} \cdot 10^{-8} / \text{mL}$), $Y2$ ($\text{gPro} \cdot \text{gGlucose}^{-1} \cdot \text{h}^{-1}$) and $Y3$ ($\text{CFU} \cdot 10^{-5} \cdot \text{gGlucose}^{-1} \cdot \text{h}^{-1}$) are yield coefficients, and α ($\text{g} \cdot \text{L}^{-1} \cdot \text{h}^{-1}$) is a constant.

The set of equations were simulated using MATLAB® (R2019a).

Three statistical criteria were used to analyze the fit of the models using experimental datasets. These parameters were the coefficient of determination (R^2), the root mean square errors (RSME), and the correction of Akaike information criterion (AICc). The expressions of these parameters are presented in Equations (8)–(11), respectively.

$$R^2 = \frac{SSR}{SST} \quad (8)$$

SSR is sum of squared regression, and SST is sum of squared total.

$$RMSE = \frac{(X - \bar{X})^T W (X - \bar{X})}{n - p} \quad (9)$$

where n represents the number of data, p the number of parameters, W the weighting matrix, and X and \bar{X} are the data and estimated data, respectively [13].

$$AICc = AIC + \frac{2p(p+1)}{n-p-1} \quad (10)$$

$$AIC = 2p + n(\ln(2\pi) + \ln(SSE) - \ln(n) + 1) \quad (11)$$

The main parameter used to determine the model that best fits the data is the AICc parameter [13]. The AIC criterion is one of the most popular for the comparison of models because it considers the number of parameters, the number of data, and the residuals, making it a parameter that balances the complexity of the model and the fit of the data [14]. Additionally, the parameter correction (AICc) gives accurate results for a larger number of datasets. Thus, the model with the lowest value for AICc is selected to represent the experimental data more adequately.

Parameter calibration was carried out in MATLAB using a particle swarm optimization (PSO) algorithm. This method, as its name implies, is inspired by the behavior of swarms of insects in nature. Thus, for a set of variables to be optimized, the method begins by placing random particles in the search space, but then a series of rules are established considering each parameter and the set of parameters (“swarm”) globally. Thus, the variables are optimized quite well, and few computational resources are spent, becoming a fast method in convergence, and simple in application [15].

3. Results

This section presents the results obtained through various simulations carried out in MATLAB. It is divided into two main sections: model calibration and model validation.

Initially, the parameters of each model were estimated (six for Model 1 and eight for Model 2) with the experimental data of two batches for each strain. Subsequently, the parameters found were used to observe the behavior of the four state variables (biomass, glucose, proteins, and spores concentrations) in two batches for the BLB1 strain and one batch for the HD1 and LIP strains. Likewise, the results obtained were compared with the experimental data. In this way, the validation of the parameters found in the calibration phase was carried out. Moreover, to compare models 1 and 2, a series of statistical parameters were calculated from which the selection of the model that best fits the experimental data is facilitated.

3.1. Model Calibration BLB1 Strain

Kinetics parameters of the *B. thuringiensis* culture were calibrated for three strains: BLB1 (Table 3), HD1 (Table 5), and LIP (Table 7). The maximum specific growth rate (μ_{\max}) was between 1.15 h^{-1} for the BLB1 strain (Model 1) and 0.39 h^{-1} for the LIP strain (Model 2). These results are within ranges similar to those reported by Holmberg and Sievanen (1980), who reported values between 1.90 and 0.17 h^{-1} [6], and Atehortúa et al. (2007), who reported values between 0.80 and 0.58 h^{-1} [16]. The death rate (k_d) was between 0.0458 (BLB1 strain) and 0.0184 h^{-1} (LIP strain), which coincided with previous results in the literature (between 0 and 0.13 h^{-1}) [6]. The yield coefficient between the biomass and the substrate (Y_1) was between $0.49 \text{ (gBiomass} \cdot \text{gGlucose}^{-1})$ and $0.96 \text{ (gBiomass} \cdot \text{gGlucose}^{-1})$ for all strains.

Table 3. Optimized parameter values from BLB1 strain.

Parameter	BLB1	
	Model 1	Model 2
$\mu_{\max} \text{ (h}^{-1}\text{)}$	1.1490	1.0720
Kc	4.7450	4.1250
Kd (h^{-1})	0.0437	0.0439
$Y_1 \text{ (gBiomass} \cdot \text{gGlucose}^{-1}\text{)}$	0.7136	0.7141
$Y_2 \text{ (gPro/gGlucose} \cdot \text{h}\text{)}$	0.0067	0.0067
$Y_3 \text{ (CFU} \cdot 10^{-5} / \text{gGlucose} \cdot \text{h}\text{)}$	0.0537	0.0524
Alpha ($\text{g/L} \cdot \text{h}\text{)}$	-	0.0001
Beta ($\text{CFU} \cdot 10^{-5} / \text{L} \cdot \text{h}\text{)}$	-	0.0001

The comparison between Models 1 and 2 and the experimental data for the BLB1 strain are shown in Figure 4. According to the figure, Models 1 and 2 did not have very noticeable differences; therefore, the alpha and beta parameters of Model 2 did not have a great impact on the modeling. Both models showed a satisfactory fit to the experimental data; however, the statistical study will give precise information on the best model. It is important to note that the quantification of the spore concentration and protein concentration are more subject to systematic error than biomass and glucose, which may explain the discrepancies between models and measurements.

Model 1 had higher values for μ_{\max} and Kc, although other parameters remained with similar values. Furthermore, for the constants alpha and beta, very low values of 0.0001 were obtained, which confirmed that both models are similar.

Table 4 presents the statistical coefficients that allowed comparing Model 1 and Model 2 for BLB1 strain. The statistical coefficients showed a good fit to the experimental data. Spores concentration was the variable with the worst fit. These results are supported by Figure 4, since the furthest experimental values of the two models can be observed in it.

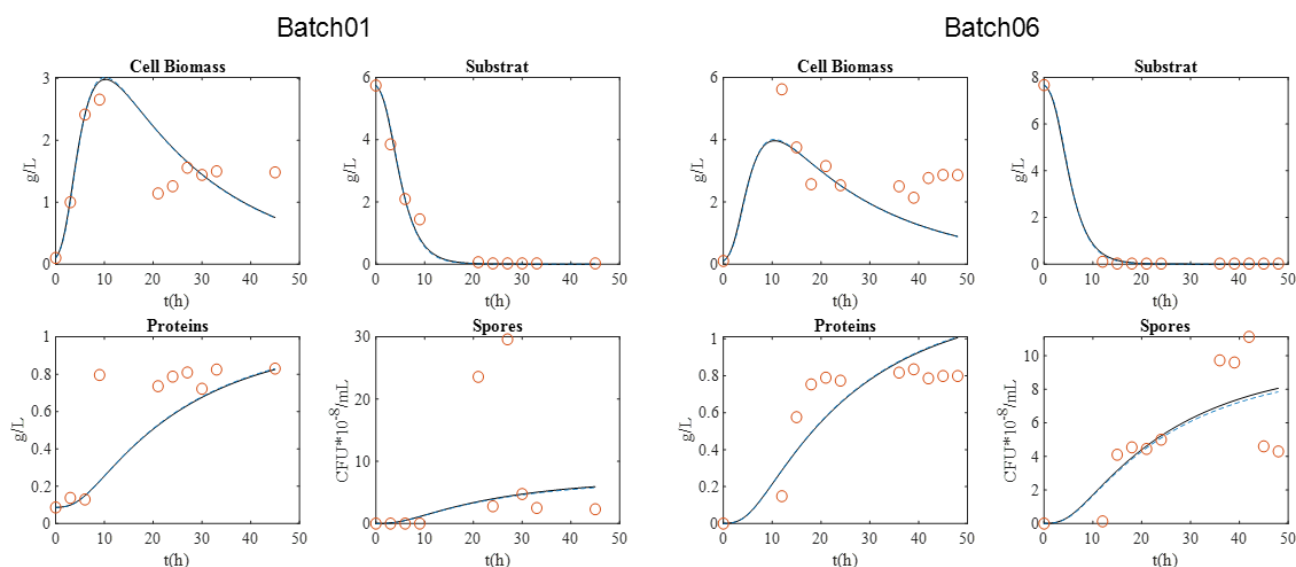


Figure 4. Calibration of the two models with the dataset from BLB1 strain. (o) Experimental data; (—) Model 1; (---) Model 2.

Table 4. Statistical evaluation of the two models with BLB1 strain.

	Model	Criterion	Biomass	Glucose	Proteins	Spores
Batch01	1	R2	0.6902	0.9863	0.7088	0.1350
		RMSE	0.4539	0.2445	0.2138	10.2994
		AICc	29.5540	17.1797	14.4991	91.9945
	2	R2	0.6935	0.9835	0.7088	0.1357
		RMSE	0.4552	0.2711	0.2125	10.3321
		AICc	149.6104	139.2478	134.3794	212.0580
Batch06	1	R2	0.5663	0.9976	0.7329	0.5756
		RMSE	1.1693	0.1154	0.1633	2.2508
		AICc	41.2816	−9.6689	−2.0279	55.6878
	2	R2	0.5686	0.9981	0.7337	0.5762
		RMSE	1.1699	0.0996	0.1638	2.2597
		AICc	96.2913	42.1035	53.0457	110.7744

As far as the determination coefficient (R2), values greater than 0.98 were observed for glucose measurements, which indicates that this variable has the best fit. However, as mentioned above, the parameter of greatest interest is the AICc since it takes into account several important aspects. The model that presented the lowest AICc values for the four variables was Model 1. This model does not include any extra constants, which makes it a less complex model than Model 2, but also predicts the behavior of the variables studied.

3.2. Model Calibration HD1 Strain

The results for the HD1 strain are shown in Figure 5 and Table 5. It was shown that there are big differences between Model 1 and Model 2. Protein concentration and spore concentration were the variables in which these differences were most visible according to Figure 5, which makes sense since the alpha and beta constants present in Model 2 have a direct influence on these two variables. Additionally, both models presented a very good fit for the biomass and substrate concentration.

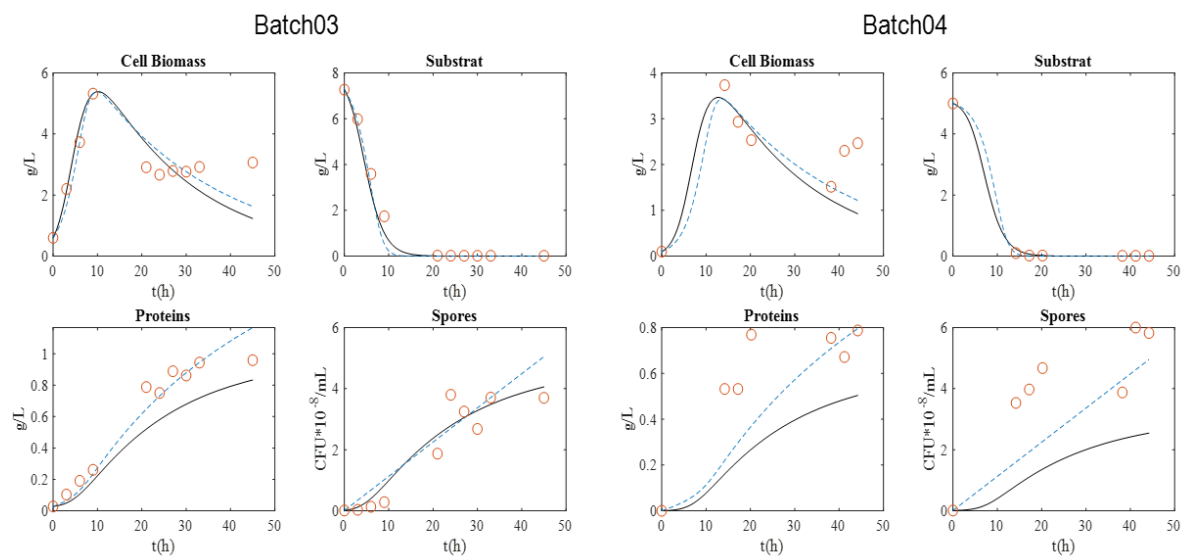


Figure 5. Calibration of the two models with the dataset from HD1 strain. (○) Experimental data; (—) Model 1; (---) Model 2.

Table 5. Optimized parameter values from HD1 strain.

Parameter	HD1	
	Model 1	Model 2
$\mu_{\max} \text{ (h}^{-1}\text{)}$	0.5985	0.4024
Kc	1.4700	0.5140
Kd (h ⁻¹)	0.0458	0.0352
Y1 gBiomass·gGlucose ⁻¹	0.9612	0.8333
Y2 (gPro/gGlucose·h)	0.0056	0.0050
Y3 (CFU*10 ⁻⁵ /gGlucose·h)	0.0281	0.0001
Alpha (g/L·h)	-	0.0062
Beta (CFU*10 ⁻⁵ /L·h)	-	0.1116

The optimized parameters showed higher values in Model 1 than in Model 2 for almost all parameters. Although the values of μ_{\max} were lower than those found for the BLB1 strain, parameters such as Y1 and alpha and beta constants were higher than those obtained with the BLB1 strain.

The results of the statistical parameters for the calibration of the HD1 strain are presented in Table 6. In a similar way to the BLB1 strain, the variable that best fits the models according to the coefficient of determination was glucose, even reaching a value of 1 for batch 4 and Model 2. In general, the R2 and RMSE coefficients showed a better fit of the models with the experimental data for the HD1 strain than the previously analyzed BLB1 strain. In fact, for HD1 strain, the experimental data of the spore concentration have a better fit than those obtained for the BLB1 strain.

Since for the HD1 strain, Model 1 showed the lowest AICc values, this model was considered as the most appropriate to predict the behavior of the HD1 strain according to the results of the calibration. This means that Model 1 showed the best parsimony.

3.3. Model Calibration LIP Strain

Figure 6 shows the results obtained for the LIP strain. Graphically, Model 1 and Model 2 showed great similarities except for protein concentration. The values obtained for the parameters and the statistical coefficients reflect these differences.

Table 6. Statistical evaluation of the two models with HD1 strain.

	Model	Criterion	Biomass	Glucose	Proteins	Spores
Batch03	1	R2	0.7086	0.9876	0.9763	0.9122
		RMSE	0.7287	0.3705	0.1677	0.4863
		AICc	39.0235	25.4968	9.6408	30.9351
	2	R2	0.7575	0.9803	0.9546	0.8486
		RMSE	0.6305	0.4203	0.0870	0.6881
		AICc	156.1279	148.0185	116.5131	157.8768
Batch04	1	R2	0.7063	0.9992	0.7036	0.73007
		RMSE	0.77276	0.0544	0.3128	2.7302
		AIC	14.6311	−22.5237	1.9751	32.3051
	2	R2	0.7666	1.0000	0.6469	0.7191
		RMSE	0.6203	0.0112	0.2140	1.5365
		AICc	−56.4420	−112.6332	−71.3404	−43.7434

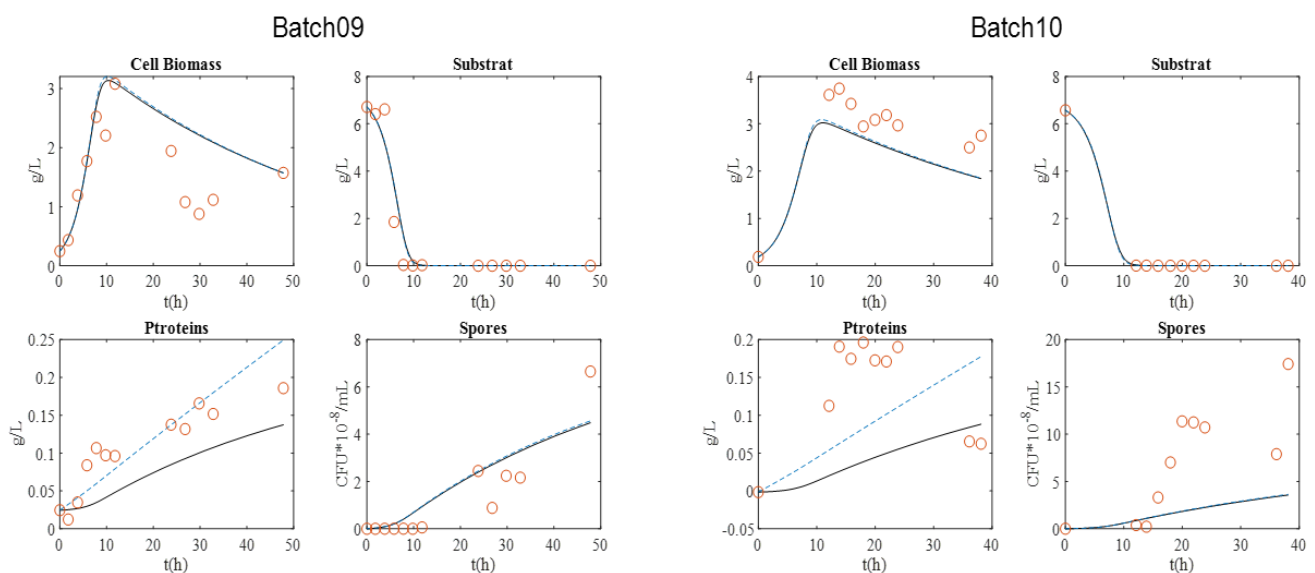
**Figure 6.** Calibration of the two models with the dataset from LIP strain. (o) Experimental data; (—) Model 1; (---) Model 2.

Table 7 summarizes the parameter values of both models. It is noteworthy that the proteins/substrate yield coefficient (Y_2) showed very low values.

Table 7. Optimized parameter values from LIP strain.

Parameter	LIP	
	Model 1	Model 2
$\mu_{\max} \text{ (h}^{-1}\text{)}$	0.3966	0.3916
Kc	0.6899	0.5794
Kd (h^{-1})	0.0189	0.0193
$Y_1 \text{ gBiomass} \cdot \text{gGlucose}^{-1}$	0.4866	0.4956
$Y_2 \text{ (gPro/gGlucose} \cdot \text{h)}$	0.0005	0.0001
$Y_3 \text{ (CFU} \cdot 10^{-5} / \text{gGlucose} \cdot \text{h)}$	0.0213	0.0218
Alpha ($\text{g/L} \cdot \text{h}$)	—	0.0042
Beta ($\text{CFU} \cdot 10^{-5} / \text{L} \cdot \text{h}$)	—	0.0002

Moreover, the calibrated parameters showed a higher value for the alpha parameter than the beta one. Therefore, the beta parameter, has a very small value and little influence on Model 2.

Table 8 indicates the values of the statistical parameters for the LIP strain. The statistical parameters showed a good fit of the models, presenting very low values of the determination coefficient only for the protein concentration in batch 10. Glucose continues to be the variable that has the best fits between two models. Additionally, as in the BLB1 and HD1 cases, Model 1 obtained the lowest values for AICc, making it the model that could best predict the behavior of the LIP strain.

Table 8. Statistical evaluation of the two models with LIP strain.

	Model	Criterion	Biomass	Glucose	Proteins	Spores
Batch09	1	R2	0.6610	0.9387	0.8130	0.7747
		RMSE	0.6795	0.7169	0.0472	0.9691
		AICc	23.7638	25.0484	−40.2561	32.2820
	2	R2	0.6653	0.9397	0.8377	0.7731
		RMSE	0.6992	0.7088	0.0289	0.9773
		AICc	59.6479	59.9742	−16.7948	67.6853
Batch10	1	R2	0.9528	1.0000	0.0002	0.6794
		RMSE	0.6082	0.0083	0.1146	7.0190
		AICc	35.4078	−50.4395	2.0181	84.3253
	2	R2	0.9507	1.0000	0.0002	0.6796
		RMSE	0.5819	0.0039	0.0920	6.9800
		AICc	154.5226	54.2584	117.6327	204.2139

3.4. Model Validation

Several datasets of each strain, different from those used in the calibration of the models, were used to validate the results obtained previously. Batch 2 and 5 were used to validate the parameters obtained for the BLB1 strain, the data from batch 7 were used for the HD1 strain, and, finally, batch 8 helped validate the parameters of the LIP strain.

3.4.1. BLB1 Strain

Figure 7 shows the results of the validation for the BLB1 strain, and Table 9 shows the respective statistical coefficients. For both experiments, the calibrated parameters fit the experimental data very well. According to Figure 7, Models 1 and 2 behaved similarly and there were no noticeable differences.

Table 9. Statistical evaluation of the two models with BLB1 strain.

	Model	Criterion	Biomass	Glucose	Proteins	Spores
Batch02	1	R2	0.1518	0.9195	0.3212	0.6722
		RMSE	0.6181	0.2109	0.4249	17.9155
		AIC	11.5082	−3.5438	6.2621	58.6431
	2	R2	0.1484	0.9077	0.3225	0.6716
		RMSE	0.6275	0.2275	0.4229	17,9704
		AICc	−56.2800	−70.4822	−61.8033	−9.3141
Batch05	1	R2	0.7510	0.9828	0.9047	0.9029
		RMSE	0.5389	0.4323	0.1302	1.0764
		AICc	32.9878	28.5794	4.5721	46.8259
	2	R2	0.7524	0.9814	0.9053	0.9029
		RMSE	0.5423	0.4433	0.1289	1.0345
		AICc	153.1159	149.0829	124.3779	166.0305

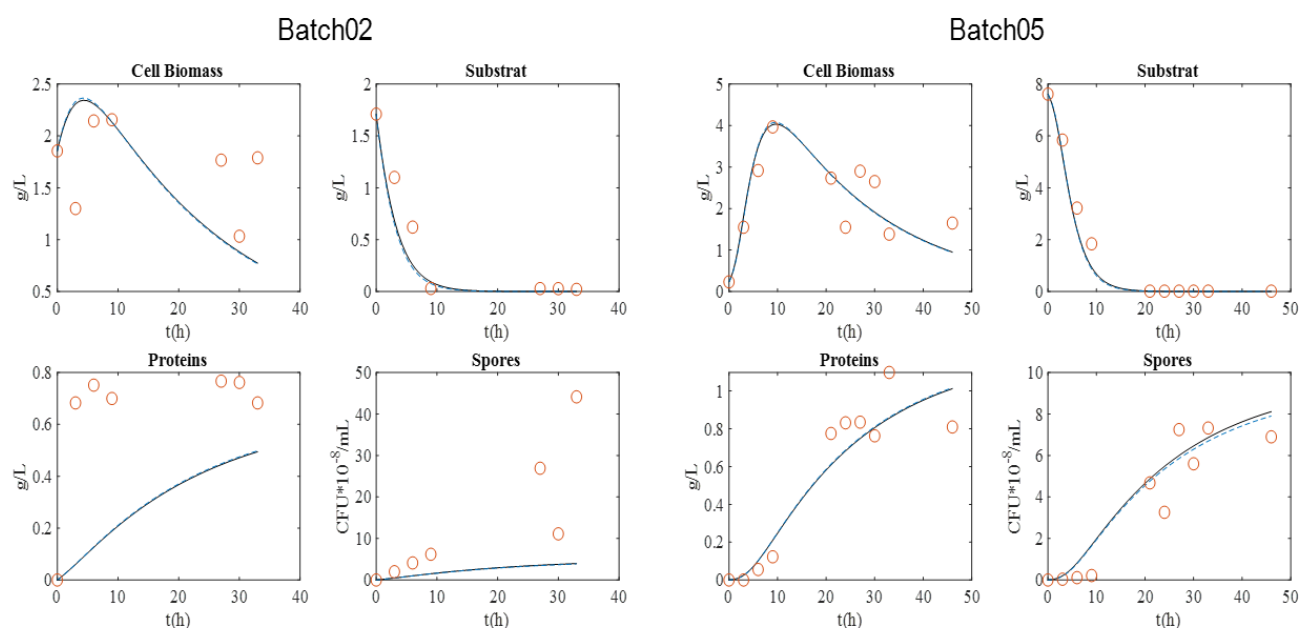


Figure 7. Validation of the two models with the dataset from BLB1 strain. (○) Experimental data; (—) for Model 1; (---) for Model 2.

Statistical analysis showed that Model 1 fit better than Model 2 because it has the lowest values of the AICc coefficient. As seen graphically, the statistical parameters showed less adjustment for some variables of batch 02 than for batch 05.

3.4.2. HD1 Strain

Data from batch 7 were used for validation of the parameters obtained in HD1 strain calibration. The results are shown in Figure 8 and Table 10. As said before, no values were recorded for the biomass concentration after exponential growth phase due to technical misplaced measurements, which is reflected in Figure 8. However, simulations showed that biomass during exponential growth phase and the other state variables fit adequately. The set of statistical coefficients that express the effectiveness of the models is expressed in Table 10.

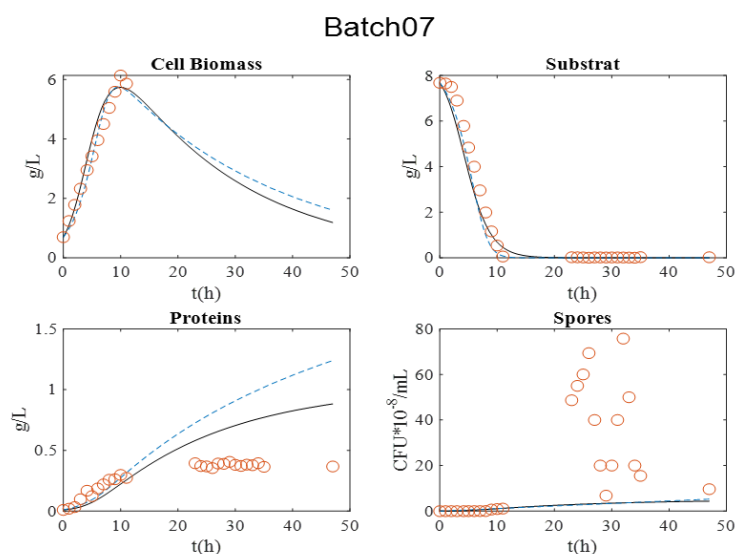


Figure 8. Validation of the two models with the dataset from HD1 strain. (○) Experimental data; (—) for Model 1; (---) for Model 2.

Table 10. Statistical evaluation of the two models with HD1 strain.

	Model	Criterion	Biomass	Glucose	Proteins	Spores
Batch07	1	R2	NC *	0.9940	0.7991	0.4551
		RMSE	NC *	0.3078	0.2263	30.1202
		AICc	NC *	−55.7705	−71.7791	182.5655
	2	R2	NC *	0.9981	0.7720	0.3628
		RMSE	NC *	0.1337	0.3701	30.1186
		AICc	NC *	−91.0931	−38.1445	190.6123

NC *: Not calculated.

Both models fit quite well for glucose concentration and followed the dynamics of spores concentration. The statistical coefficients showed the worst results for spores. As demonstrated previously, according to the AICc criterion, Model 1 should be the one used to represent the data of the HD1 strain.

3.4.3. LIP Strain

Figure 9 show the results of the validation for the LIP strain. Similar to batch 7 (HD1 strain), batch 8, which corresponds to the LIP strain, showed a biomass measurement problem. However, glucose concentration was well represented by the two models. Although the models followed the dynamics for the concentration in proteins and spores, a slight lag was evident for the spores.

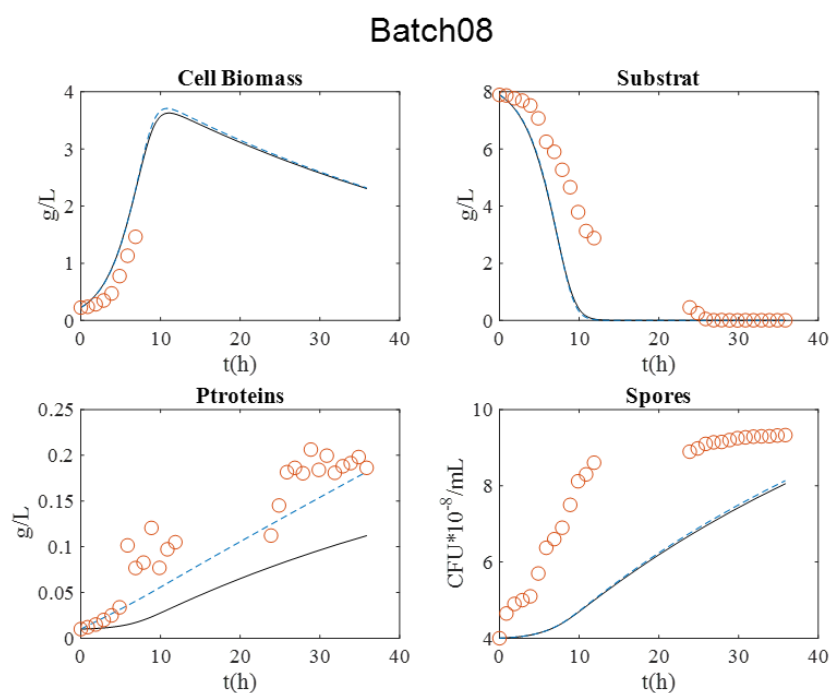
**Figure 9.** Validation of the two models with the dataset from LIP strain. (o) Experimental data; (—) Model 1; (---) Model 2.

Table 11 presents results for statistics parameters in LIP validation. As for the other two strains, the glucose data showed the best fit. However, the coefficient of determination for proteins and spores showed a good fit of the models. As in all the cases studied in this report, the most suitable model to predict and represent the experimental data is Model 1, according to the AICc criterion.

Table 11. Statistical evaluation of the two models with LIP strain.

	Model	Criterion	Biomass	Glucose	Proteins	Spores
Batch08	1	R2	NC *	0.9883	0.8321	0.7054
		RMSE	NC *	0.3716	0.0817	2.4370
		AICc	NC *	−45.9879	−124.7646	51.8161
	2	R2	NC *	0.9878	0.8937	0.7042
		RMSE	NC *	0.3813	0.0351	2.4099
		AICc	NC *	−36.5917	−160.6215	59.2837

NC *: Not calculated.

4. Conclusions

The objectives of approach were to model bioperformances (vegetative cell, spore, substrate, and protein) considering different *B. thuringiensis* ssp. *kurstaki* strains and successive culture phases (oxidative growth, limitation and sporulation, protein release). Our overarching aim to estimate total proteins production (mainly composed of δ -endotoxin) was successfully achieved. Initially, the bibliographic research allowed understanding of the context and the different phenomena involved in the study of the *B. thuringiensis* culture, such as the particular life cycle of these microorganisms and the importance of the endotoxins produced.

B. thuringiensis is an important microorganism for the biopesticide market worldwide. The experimental simulations developed in the present study and based on *B. thuringiensis* cultures made it possible to analyze the behavior of the concentration in biomass, substrate, proteins, and spores and adjust two models to the experimental datasets. The calibration of both models allowed to calculate the kinetic parameters of the culture, and the experimental data presented a good fit. Likewise, the models were validated in a satisfactory way.

For the selection of the best model, the AICc criterion was used, which, for all batches, showed better results for Model 1 due to its parsimony. Additionally, although the BLB1 strain showed the highest maximum specific growth rate (μ_{max}), the HD1 strain presented the highest biomass/substrate yield coefficient values (Y_1), in opposition to the LIP strain which presented the lowest values for this yield. As for the production of proteins, mainly used for insecticidal toxicity, the BLB1 strain presented the highest concentration and proteins/substrate yield coefficient (Y_2), while the LIP strain showed the lowest values for this yield.

Author Contributions: Conceptualization, C.A.A.-L. and L.F.; methodology, T.S.M. and C.A.A.-L.; software, T.S.M. and C.A.A.-L.; validation, T.S.M. and C.A.A.-L.; formal analysis, T.S.M., N.A., S.R., M.K., L.F. and C.A.A.-L.; investigation, T.S.M. and C.A.A.-L.; resources, N.A., S.R., M.K., J.S., J.A., J.C., N.B. and L.F.; data curation, N.A., S.R., M.K., J.S., J.A., J.C., N.B. and L.F.; writing—original draft preparation, T.S.M. and C.A.A.-L.; writing—review and editing, T.S.M., N.A., S.R., M.K., L.F. and C.A.A.-L.; visualization, T.S.M. and C.A.A.-L.; supervision, N.A., S.R., M.K., L.F. and C.A.A.-L.; project administration, S.R. and L.F.; funding acquisition, S.R. and L.F. All authors have read and agreed to the published version of the manuscript.

Funding: This work was conducted under the IPM-4-Citrus project, funded by the European Commission (ID:734921; Period: From 1 April 2017 to 31 March 2021; <https://cordis.europa.eu/project/rcn/207633/factsheet/en>, accessed on 19 November 2021).

Institutional Review Board Statement: Not applicable.

Informed Consent Statement: Not applicable.

Conflicts of Interest: The authors declare no conflict of interest.

References

1. Schnepf, E.; Crickmore, N.; Van Rie, J.; Lereclus, D.; Baum, J.; Feitelson, J.; Zeigler, D.R.; Dean, D.H. Bacillus thuringiensis and Its Pesticidal Crystal Proteins. *Microbiol. Mol. Biol. Rev.* **1998**, *62*, 775–806. [\[CrossRef\]](#) [\[PubMed\]](#)
2. Iriarte, J.; Porcar, M.; Lecadet, M.-M.; Caballero, P. Isolation and Characterization of Bacillus thuringiensis Strains from Aquatic Environments in Spain. *Curr. Microbiol.* **2000**, *40*, 402–408. [\[CrossRef\]](#) [\[PubMed\]](#)
3. Rowe, G.E.; Margaritis, A. Bioprocess design and economic analysis for the commercial production of environmentally friendly bioinsecticides from *Bacillus thuringiensis* HD-1kurstaki. *Biotechnol. Bioeng.* **2004**, *86*, 377–388. [\[CrossRef\]](#) [\[PubMed\]](#)
4. El Khoury, M.; Azzouz, H.; Chavanieu, A.; Abdelmalak, N.; Chopineau, J.; Awad, M.K. Isolation and characterization of a new *Bacillus thuringiensis* strain Lip harboring a new cry1Aa gene highly toxic to *Ephestia kuehniella* (Lepidoptera: Pyralidae) larvae. *Arch. Microbiol.* **2014**, *196*, 435–444. [\[CrossRef\]](#) [\[PubMed\]](#)
5. Navarro-Mtz, A.K.; Pérez-Guevara, F. Construction of a biodynamic model for Cry protein production studies. *AMB Express* **2014**, *4*, 79. [\[CrossRef\]](#) [\[PubMed\]](#)
6. Holmberg, A.; Sievanen, R. Fermentation of Bacillus thuringiensis for Exotoxin Production: Process Analysis Study. *Biotechnol. Bioeng.* **1980**, *22*, 1707–1724. [\[CrossRef\]](#)
7. Rivera, D.; Margaritis, A.; de Lasa, H. A sporulation kinetic model for batch growth of *B. thuringiensis*. *Can. J. Chem. Eng.* **1999**, *77*, 903–910. [\[CrossRef\]](#)
8. Popovic, M.K.; Liu, W.-M.; Iannotti, E.L.; Bajpai, R.K. A Mathematical Model for Vegetative Growth of *Bacillus Thuringiensis*. *Eng. Life Sci.* **2001**, *1*, 85–90. [\[CrossRef\]](#)
9. Saadaoui, I.; Rouis, S.; Jaoua, S. A new Tunisian strain of Bacillus thuringiensis kurstaki having high insecticidal activity and δ -endotoxin yield. *Arch. Microbiol.* **2009**, *191*, 341–348. [\[CrossRef\]](#) [\[PubMed\]](#)
10. Carozzi, N.B.; Kramer, V.C.; Warren, G.W.; Evola, S.; Koziel, M.G. Prediction of insecticidal activity of *Bacillus thuringiensis* strains by polymerase chain reaction product profiles. *Appl. Environ. Microbiol.* **1991**, *57*, 3057–3061. [\[CrossRef\]](#) [\[PubMed\]](#)
11. Sarrafzadeh, M.H.; Guiraud, J.P.; Lagneau, C.; Gaven, B.; Carron, A.; Navarro, J.-M. Growth, Sporulation, δ -Endotoxins Synthesis, and Toxicity During Culture of *Bacillus thuringiensis* H14. *Curr. Microbiol.* **2005**, *51*, 75–81. [\[CrossRef\]](#) [\[PubMed\]](#)
12. Bradford, O.F. Adaptation of the Bradford protein assay to membrane-bound proteins by solubilizing in glucopyranoside detergents. *Anal. Biochem.* **1987**, *162*, 11–17.
13. Robles-Rodriguez, C.; Bideaux, C.; Gaucel, S.; Laroche, B.; Gorret, N.; Aceves-Lara, C. Reduction of metabolic models by polygons optimization method applied to Bioethanol production with co-substrates. *IFAC Proc. Vol.* **2014**, *47*, 6198–6203. [\[CrossRef\]](#)
14. Burnham, K.P.; Anderson, D.R. Multimodel Inference: Understanding AIC and BIC in Model Selection. *Sociol. Methods Res.* **2004**, *33*, 261–304. [\[CrossRef\]](#)
15. Robles-Rodriguez, C.E.; Bideaux, C.; Roux, G.; Molina-Jouve, C.; Aceves-Lara, C.A. Soft-Sensors for Lipid Fermentation Variables Based on PSO Support Vector Machine (PSO-SVM). In Proceedings of the 13th International Conference on Distributed Computing and Artificial Intelligence, Sevilla, Spain, 1–3 June 2016; pp. 175–183.
16. Atehortúa, P.; Álvarez, H.; Orduz, S. Modeling of growth and sporulation of Bacillus thuringiensis in an intermittent fed batch culture with total cell retention. *Bioprocess Biosyst. Eng.* **2007**, *30*, 447–456. [\[CrossRef\]](#) [\[PubMed\]](#)